Indonesian Journal of Aerospace Vol. 23 No. 1 Juni 2025 : pp 23 – 44 (Ardiansyah et al.)
DOI: 10.59981/ijoa.2025.9041
https://ejournal.brin.go.id/ijoa/

Guidance and Control System Design of a Surface-to-Air Missile Based on 122 mm Rocket

Alvin Ardiansyah[1], Y. H. Yogaswara [2,3], Rianto Adhy Sasongko[1], Taufiq Mulyanto[1]

[1]Faculty of Mechanical and Aerospace Engineering, Bandung Institute of Technology, Indonesia
[2]Faculty of Defense Engineering and Technology, Indonesia Defense University, Indonesia
[3]Research and Development Service, Indonesian Air Force, Indonesia
e-mail: yh.yogaswara@idu.ac.id

Received: 23-12-2024 Accepted: 03-09-25 Published: 05-10-2025

Abstract

This paper applies and analyzes the design of a proportional navigation guidance and control system for a 122 mm rocket platform. The research involves modeling missile dynamics, guidance systems, and control systems. The missile dynamics model relies on the 6 DOF (Degrees of Freedom) equation for a rigid body, with aerodynamic data obtained from the Missile Datcom program. The propulsion model is generated by a generic thrust profile of a 122 mm unguided rocket. The guidance system model is based on the proportional navigation guidance law, and the control system model employs the Linear Quadratic Regulator (LQR) method. Modeling is conducted using Simulink software, and simulations encompass various scenarios. The analysis considers aspects such as missile trajectory, acceleration command, actual acceleration, control surface deflection, and the time required to hit the target. The simulation results indicate the missile's capability to intercept targets under numerous conditions, although limitations are observed in specific target scenarios where interception is not achievable.

Keywords**:** *proportional navigation, flight control, flight dynamics, missile, guidance.*

1. Introduction

Indonesia possesses various Surface-to-Air Missile (SAM) systems designed to safeguard its airspace. Despite the presence of these SAMs, Indonesia's air defense capabilities remain insufficient. The detection and recognition of airborne threats are facilitated by the National Air Defense Command (Hanud Kohanudnas) radar, strategically deployed throughout the country. However, the current enforcement efforts are deemed inadequate, primarily attributed to the limited number and positioning of combat fighter aircraft for responsive action, along with the absence of medium-range missiles as effective tools (Membangun Kembali Satuan Rudal TNI AU, 2021).

The large number of missiles that Indonesia needs has encouraged the development of domestically made missiles. Missile development is needed to reduce dependence on other countries for missile needs. Indonesia has several rockets that have the potential to be developed into SAM. One of those rockets is 122 mm calibre rocket based on reference (Cahyono, Navalino, & Yogaswara, 2021). Research on the development of a rocket to guided missile based on a 122mm calibre has been conducted, and the results show that this rocket is capable of being developed into a surface-to-air missile (Y. H. Yogaswara, 2020). The research conducts a simulation of missile flight dynamics as a point mass. This simulation was also carried out by reference (Ardiansyah, 2022). In this research, fin design was also carried out. These researches are still in conceptual design, which requires a number of design iterations to achieve a balance of emphasis from the diverse inputs and outputs (Fleeman, 2001).

The most important aspect of a missile system, which turns a rocket into a guided missile, is the guidance, navigation, and control system. Guidance is the process by which a missile steers, or is steered, to a target. A guided missile is guided according to a specific guidance law (Siouris, 2004). In this research, the guidance law used is proportional

navigation. The navigation system is a system for determining current position or movement, such as missile velocity, line of sight rate, and flight path angle. The control system refers to the manipulation of forces by changing the control surfaces, in this case, the missile fins, to execute guidance commands (Siouris, 2004). In this research, a PI controller is used, which contains proportional gain and integral gain, as the name suggests. To obtain the gains, it uses the LQR method.

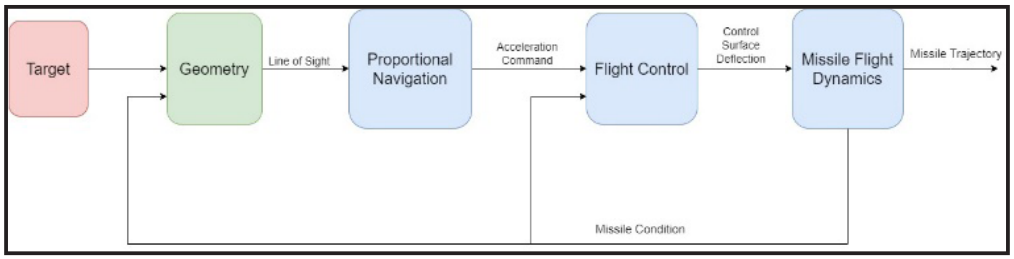

Figure 1: Integration of Navigation, Guidance, Control, and Dynamics System.

The integration of all these systems is illustrated in Figure 1. In this figure, the engagement process is described by the block diagram. The diagram depicts that initially, the target and missile positions are considered by the navigation system, i.e., geometry, resulting in the line of sight computed by the seeker. The line of sight is then utilized as an input for proportional navigation to compute the acceleration command. This process is carried out by the onboard computer. Subsequently, the acceleration command is employed to determine the deflection of the control surfaces through flight control. The control surfaces are four canards, which translate to virtual deflection: aileron, elevator, and rudder. The alteration in the control surfaces' deflection influences the missile trajectory, and this is computed through the missile flight dynamics. The missile trajectory will intercept the target trajectory, which is due to the constant bearing of the trajectories.

In a constant bearing course, the alignment between the target and the missile remains fixed in space, maintaining parallel lines of sight throughout the engagement. It means that the angle of the line of sight remains unchanged. Illustrated in Figure 2, the concept of a constant bearing course ensures interception as long as there is a positive closing velocity between the missile and the target. Proportional navigation leverages this concept by driving the rate of change of the line of sight towards zero (Lukenbill, 1990).

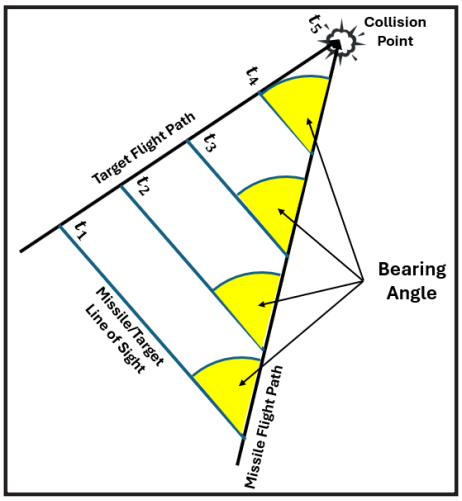

Figure 2: Constant Bearing Course.

This paper primarily focuses on the construction of a comprehensive missile guidance and control system. It encompasses crucial elements such as the mathematical model of flight dynamics for accurately representing missile motion, the development of a missile guidance system using Matlab Simulink software, the design of an efficient missile control system, seamless integration of these systems, simulation of the missile trajectory, and a thorough analysis of the obtained results.

Methodology

This section provides an overview of proportional navigation, geometry engagement, missile configuration, missile equation of motion, LQR method, and numerical modeling of flight simulation using MATLAB Simulink software.

2.1. Proportional Navigation

Proportional navigation missiles are guided by either reflected or emitted energy from the target. A passive missile relies on energy emitted by the target, such as infrared (IR), electro-optical (EO), or radio frequency (RF) emissions, for guidance. Conversely, an active missile emits an RF signal to track the target. In both scenarios, a seeker captures this energy to track the target (Costello, 1995). Proportional Navigation (PN) was selected as the primary guidance law due to its computational simplicity, effectiveness against non-maneuvering and moderately maneuvering targets, and widespread use in tactical missile systems. Compared to other guidance laws such as Pure Pursuit (PP) and Augmented Proportional Navigation (APN), PN provides a balance between robustness and implementation feasibility.

Proportional navigation guidance is based on the recognition that if two bodies are closing on each other, they will eventually intercept if the line of sight (LOS) between them does not rotate relative to inertial space (Siouris, 2004). In a proportional navigation system, the missile stays on a trajectory with a constant bearing angle to the target, as shown in Figure 3.

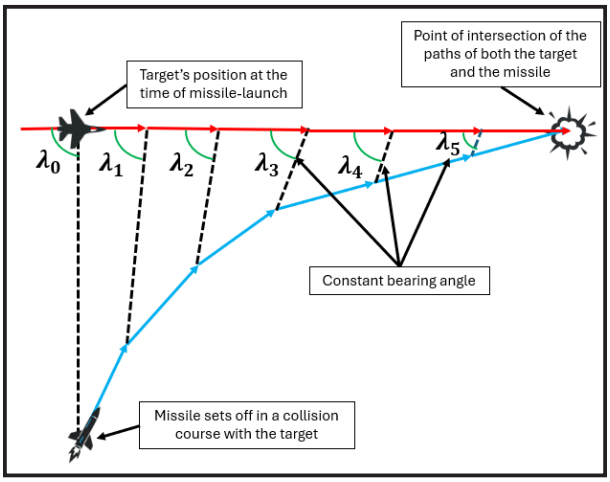

Figure 3: Proportional Navigation Illustration.

The direction of proportional navigation is perpendicular to the missile velocity vector. The equation of proportional navigation is as follows.

$$a_n = NV_m\dot{\sigma} \tag{1}$$
$$N = \frac{\dot{\gamma}_m}{\dot{\sigma}}$$

The result of proportional navigation is the commanded lateral acceleration (a_n). The proportionality factor consists of the navigation constant (N), missile velocity (V_m), and line of sight rate $(\dot{\sigma})$. The navigation constant (N) is based on the missile's acceleration requirements and varies depending on target maneuvers and other system-induced tracking error sources. To minimize the missile acceleration requirement, values of N between 3 and 5 are typically used to achieve an acceptable miss distance intercept (Siouris, 2004). The navigation constant also represents the sensitivity of the missile system (Lukenbill, 1990). It is described as the ratio of the flight path angle rate $(\dot{\gamma}_m)$ and LOS rate.

2.2. Geometry Engagement

Modelling proportional navigation guidance requires the engagement geometry in three-dimensional space and the object represented by rigid bodies. Geometry is used to determine the missile acceleration command from proportional navigation in three-dimensional space. The engagement geometry that must be known is the velocity relationship, line of sight

angle, and flight path angle (Costello, 1995).

1) Velocity relationship

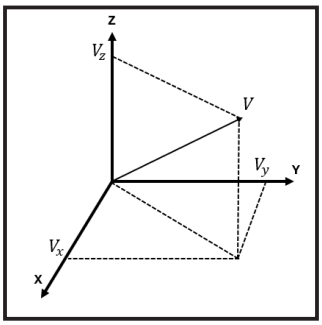

Figure 4: Velocity Relationship.

The missile and target velocity (V_m, V_t) are presented in vector form, and the velocity magnitude is written below.

$$V_m = \sqrt{V_{mx}^2 + V_{my}^2 + V_{mz}^2} \tag{2}$$

$$V_t = \sqrt{V_{tx}^2 + V_{ty}^2 + V_{tz}^2} \tag{3}$$

The subscripts (x, y, z) denote the velocity component direction.

2) Line of sight angle

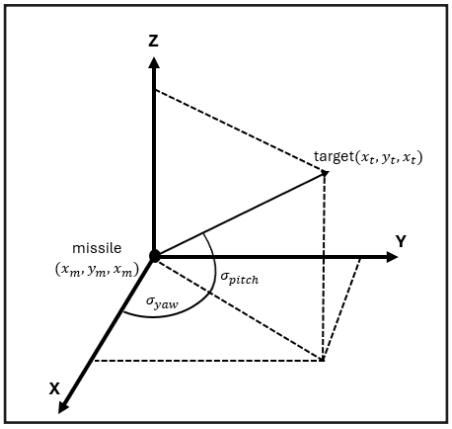

Figure 5: Pitch and Yaw Line of Sight Angle Definitions.

The line-of-sight equation between missile and target is divided into two directions, pitch and yaw direction $(\sigma_{pitch}, \sigma_{yaw})$. And these equations are shown below.

$$\sigma_{pitch} = \tan^{-1}\left[\frac{z_t - z_m}{\sqrt{(x_t - x_m)^2 + (y_t - y_m)^2}}\right] \tag{4}$$

$$\sigma_{yaw} = \tan^{-1}\left[\frac{(y_t - y_m)}{(x_t - x_m)}\right] \tag{5}$$

Where (x_m, y_m, z_m) and (x_t, y_t, z_t) denote the position of the missile and target.

3) Flight path angle

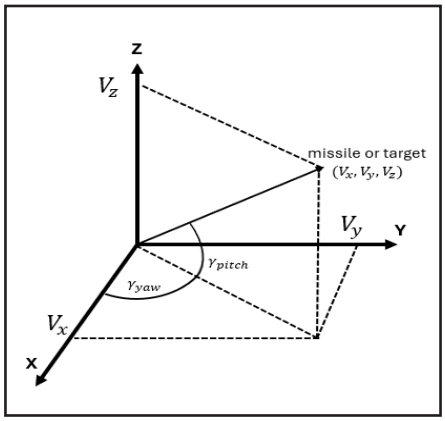

Figure 6: Target and Missile Flight Path Angle Definitions.

The flight path angle of the missile was also divided into two directions, pitch and yaw direction $(\gamma_{m_{pitch}}, \gamma_{m_{yaw}})$. Mathematically,

$$\gamma_{m_{pitch}} = \tan^{-1}\left[\frac{V_{mz}}{\sqrt{V_{mx}^2 + V_{my}^2}}\right] \tag{6}$$

and

$$\gamma_{m_{yaw}} = \tan^{-1}\left[\frac{V_{my}}{V_{mx}}\right] \tag{7}$$

4) Velocity and Acceleration

The velocity and acceleration are also defined in two orthogonal planes: the pitch plane and the yaw plane. The missile velocity in the pitch plane $(V_{m_{pitch}})(V_{m_{pitch}})$ is

$$V_{m_{pitch}} = V_m \cos\left(\gamma_{m_{yaw}} - \sigma_{yaw}\right) \tag{8}$$

From the basic relationship, the missile acceleration and the missile pitch acceleration $\left(A_{m_{pitch}}\right)$ is defined as,

$$A_{m_{pitch}} = V_{m_{pitch}} . \dot{\gamma}_{m_{pitch}} \tag{9}$$

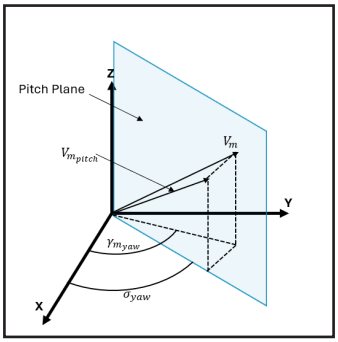

Figure 7: Pitch Plane Definition.

Where $\dot{\gamma}_{m_{pitch}}$ is the rate of change of the missile's flight path angle in the pitch plane. This acceleration vector is then decomposed into its Cartesian coordinate system components. Assuming that the pitch acceleration vector is perpendicular to the vertical line of sight vector between the missile and target, Figure 7 shows the orientation of the acceleration components. From this figure, the following relationships are obtained:

$$\begin{aligned} \ddot{x}_{m_{pitch}} &= -\left(A_{m_{pitch}} . \sin\sigma_{pitch}\right)\cos\sigma_{yaw} \\ \ddot{y}_{m_{pitch}} &= -\left(A_{m_{pitch}} . \sin\sigma_{pitch}\right)\sin\sigma_{yaw} \\ \ddot{z}_{m_{pitch}} &= A_{m_{pitch}} . \cos\sigma_{pitch} \end{aligned} \tag{10}$$

Where $(\ddot{x}_{m_{pitch}}, \ddot{y}_{m_{pitch}}, \ddot{z}_{m_{pitch}})$ are the acceleration in the pitch plane.
The velocity in the yaw plane $\left(V_{m_{yaw}}\right)$ is simply

$$V_{m_{yaw}} = V_m \cdot \cos\gamma_{m_{pitch}} \tag{11}$$

From the basic missile acceleration relationship, the missile yaw acceleration $\left(A_{m_{yaw}}\right)$ is defined as

$$A_{m_{yaw}} = V_{m_{yaw}} \cdot \dot{\gamma}_{m_{yaw}} \tag{12}$$

Where $\dot{\gamma}_{m_{yaw}}$ $\dot{\gamma}_{m_{yaw}}$ is the rate of change of missile flight path angle in the yaw plane. The missile yaw acceleration components are depicted in Figure 2-6 and are given mathematically as

$$\ddot{x}_{m_{yaw}} = -A_{m_{yaw}} \cdot \sin\sigma_{yaw} \tag{13}$$

$$\ddot{y}_{m_{yaw}} = A_{m_{yaw}} \cdot \cos\sigma_{yaw} \tag{14}$$

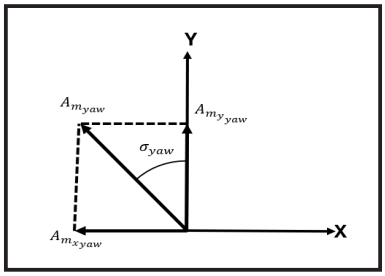

Figure 8 Yaw: Plane Acceleration Command.

Where $(\ddot{x}_{m_{yaw}}, \ddot{y}_{m_{yaw}})$ are the acceleration in the yaw plane
Given the missile acceleration components in both the pitch and yaw planes, the total missile acceleration components are

$$\begin{aligned} \ddot{x}_m &= \ddot{x}_{m_{pitch}} + \ddot{x}_{m_{yaw}} \\ \ddot{y}_m &= \ddot{y}_{m_{pitch}} + \ddot{y}_{m_{yaw}} \\ \ddot{z}_m &= \ddot{z}_{m_{pitch}} \end{aligned} \tag{15}$$

2.3. Missile Configuration

The airframe used in this paper is based on the reference (Ardiansyah, 2022). The airframe is a 122 mm rocket airframe, which has been modified by adding fins. The following is a 122 mm rocket airframe that was modified for use in this research.

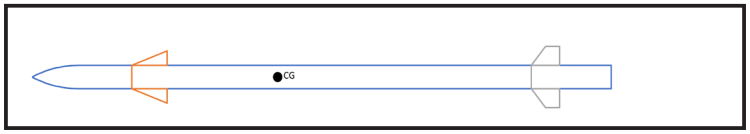

Figure 9: 122 Mm Rocket Airframe.

The control plane used in this missile is the canard, namely, the fin in front of the CG. The missile employs the Skid-to-Turn (STT) control method due to its more straightforward implementation compared to the Bank-to-Turn (BTT) method. STT directly commands lateral acceleration without requiring coordinated roll maneuvers, whereas BTT necessitates an additional roll control system. The configuration of this fin is positive (+), making it easier for the missile to maneuver using a skid-to-turn (STT) scheme. The control plane deflection used is the virtual deflection, which regulates the yaw, pitch, and roll of the missile, also known as the rudder, elevator, and aileron. The deflection of the control plane is defined as follows (Siouris, 2004).

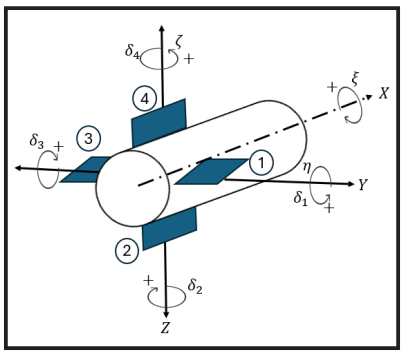

Figure 10: Missile Fin Deflection Definition.

Aileron deflection:

$$\delta_a = -\frac{1}{4}(\delta_1 + \delta_2 + \delta_3 + \delta_4) \tag{2.16}$$

Elevator deflection*:*

$$\delta_e = \frac{1}{2}(\delta_1 - \delta_3) \tag{2.17}$$

Rudder deflection*:*

$$\delta_r = \frac{1}{2}(\delta_2 - \delta_4) \tag{2.18}$$

The fin definition and deflection direction from the above equation are in accordance with Figure 10.

The propulsion profile used is the generic 122 mm caliber rocket profile synthesized to achieve flight performance close to its characteristic features for 6000 newton average thrust and 5-second burn time. The aerodynamic data were obtained using the Missile Datcom program (Rosema, Doyle, Underwood, & Auman, 2011) with the previously mentioned missile configuration. The aerodynamic data obtained from Missile Datcom include three force coefficients, three moment coefficients, stability derivatives, and control derivatives. The missile has met the stability criteria according to reference (Mulder, Staveren, van der Vaart, & Weerdt, 2011).

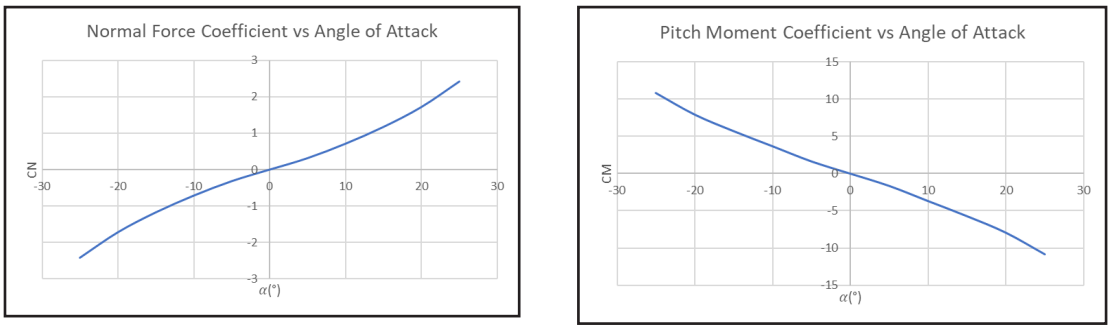

(a) (b)

Figure 11: (a) Normal Force Coefficient, (b) Pitch Moment Coefficient.

Figure 11 shows the normal coefficient and pitch moment coefficient with respect to the angle of attack that Missile Datcom has calculated. The atmospheric model used in the numerical model is based on the standard atmosphere, also known as the International Standard Atmosphere (ISA).

2.4. Missile Equation of Motion

The missile equation of motion uses the rigid body equation of motion and has six degrees of freedom (6-DOF). The six degrees of freedom consist of (1) three translations (u, v, w),

and (2) three rotations (p, q, r), along and about the missile (X_b, Y_b, Z_b) axes. The equation is derived from reference (Siouris, 2004), (Hibbeler, 2010), and (Meriam, Kraige, & Bolton, 2015). The missile's linear equations of motion are shown below.

$$\sum \Delta F_x = m(\dot{u} + wq - vr)$$
$$\sum \Delta F_y = m(\dot{u} + ur - wp) \quad (19)$$
$$\sum \Delta F_z = m(\dot{w} + vp - uq)$$

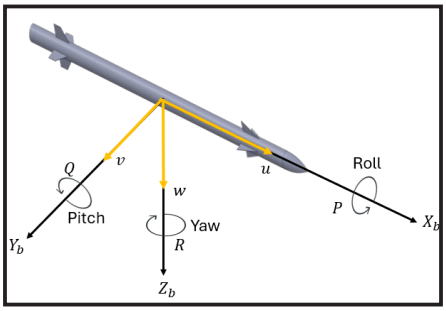

Figure 12: Representation of the Missile's Six Degrees of Freedom.

The left-hand side of the equation above is the external forces, and the missile's angular equations of motion are shown below (Siouris, 2004):

$$\sum \Delta L = I_x \dot{p}$$
$$\sum \Delta M = I_y \dot{q} + pr(I_x - I_y) \quad (20)$$
$$\sum \Delta N = I_y \dot{r} + pq(I_y - I_x)$$

Three forces are acting on the missile: the gravitational force $(\boldsymbol{F_g})$, thrust force $(\boldsymbol{F_T})$ and aerodynamic force $(\boldsymbol{F_a})$. For the moment, there is only an aerodynamic moment $(\boldsymbol{M_a})$ affecting the missile. Thus, the external forces and moment are the summation of these forces and moments in vector forms:

$$\sum \Delta \boldsymbol{F} = \boldsymbol{F_g} + \boldsymbol{F_T} + \boldsymbol{F_a} \quad (21)$$
$$\sum \Delta \boldsymbol{M} = \boldsymbol{M_a} \quad (22)$$

The gravity forces are determined by the missile's weight, the thrust forces are obtained from experimental data, and the aerodynamic forces and moments are obtained from Missile Datcom.

The equations of motion above are still in nonlinear form; thus, they need to be linearized. The linearized equations of motion are used to design the controller. The linearized equations of motion are written in state-space form below.

$$\dot{\boldsymbol{x}} = \boldsymbol{Ax} + \boldsymbol{Bu} \quad (23)$$
$$\boldsymbol{y} = \boldsymbol{Cx} + \boldsymbol{Du} \quad (24)$$

Where $\boldsymbol{x}$ is referred to as the state vector, $\boldsymbol{u}$ is the input, and $\boldsymbol{y}$ is the output. The state vector and output vector of the missile used in this research are,

$$\boldsymbol{x}^T = [\phi \quad \theta \quad \psi \quad p \quad q \quad r \quad u \quad v \quad w] \qquad \boldsymbol{y}^T = [a_{y_b} \quad a_{z_b}] \quad (25)$$

The state vector comprises Euler angles, body rate, and missile velocity in the body frame. The output vector consists of the missile's lateral acceleration in both the pitch and yaw planes.

2.5. LQR Method

LQR or Linear Quadratic Regulator is one of the control systems design methods. It provides optimally controlled feedback gains to enable the design of closed-loop systems that are stable and high-performance. The Linear Quadratic Regulator (LQR) was chosen due to its optimal control properties, ease of implementation, and ability to handle multi-variable state feedback efficiently. While nonlinear control techniques, such as adaptive control or robust H-infinity control, could provide better performance under uncertain conditions, LQR ensures optimal trade-offs between control effort and tracking performance, given the linearized missile dynamics model.

The state-space equation of the model is as shown in equations (23) and (24) with state vector and output vector in equation (25). It determines the matrix $\boldsymbol{KK}$ of the optimal control vector.

$$\boldsymbol{u}(t) = -\boldsymbol{K}\boldsymbol{x}(t) \tag{26}$$

To minimize the performance index

$$J = \int_0^\infty (\boldsymbol{x}^T\boldsymbol{Q}\boldsymbol{x} + \boldsymbol{u}^T\boldsymbol{R}\boldsymbol{u})dt \tag{27}$$

Where $\boldsymbol{Q}$ is a positive-definite (or positive-semidefinite) Hermitian or real symmetric matrix and $\boldsymbol{R}$ is a positive-definite Hermitian or real symmetric matrix (Ogata, 2010).

The system used in this paper has no integrator; the idea of designing that system is to insert an integrator in the feedforward path between the error comparator and the system, as shown in Figure 13.

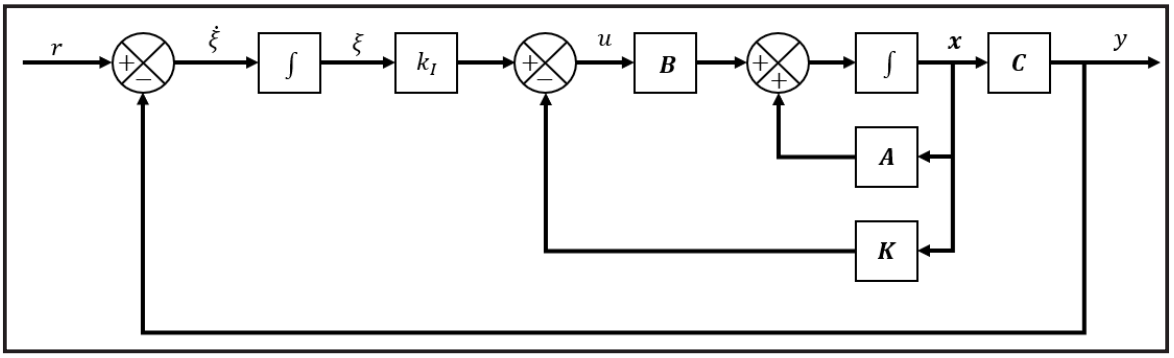

Figure 13: Block Diagram for Tracking Controller.

The block diagram above can be described by the state error equation below.

$$\dot{\boldsymbol{e}} = \hat{\boldsymbol{A}}\boldsymbol{e} + \hat{\boldsymbol{B}}\boldsymbol{u}_{\boldsymbol{e}} \tag{28}$$

Where $\hat{\boldsymbol{A}}$ and $\hat{\boldsymbol{B}}$ are the augmented matrix.

$$\hat{\boldsymbol{A}} = \begin{bmatrix} \boldsymbol{A} & \boldsymbol{0} \\ -\boldsymbol{C} & \boldsymbol{0} \end{bmatrix}$$

$$\hat{\boldsymbol{B}} = \begin{bmatrix} \boldsymbol{B} \\ -\boldsymbol{D} \end{bmatrix} \tag{29}$$

And the input is,

$$\boldsymbol{u}_{\boldsymbol{e}} = -\hat{\boldsymbol{K}}\boldsymbol{e} \tag{30}$$

Where

$$\hat{\boldsymbol{K}} = [\boldsymbol{K}_{\boldsymbol{p}} \vdots -\boldsymbol{K}_{\boldsymbol{I}}] \tag{31}$$

The gain matrix is composed of the proportional and integral gains. The proportional gain is used to calculate the control signal from the state-feedback error. The integral gain is used to calculate the control signal from the lateral acceleration error. Figure 14 shows the control system and all the state variables used for feedback.

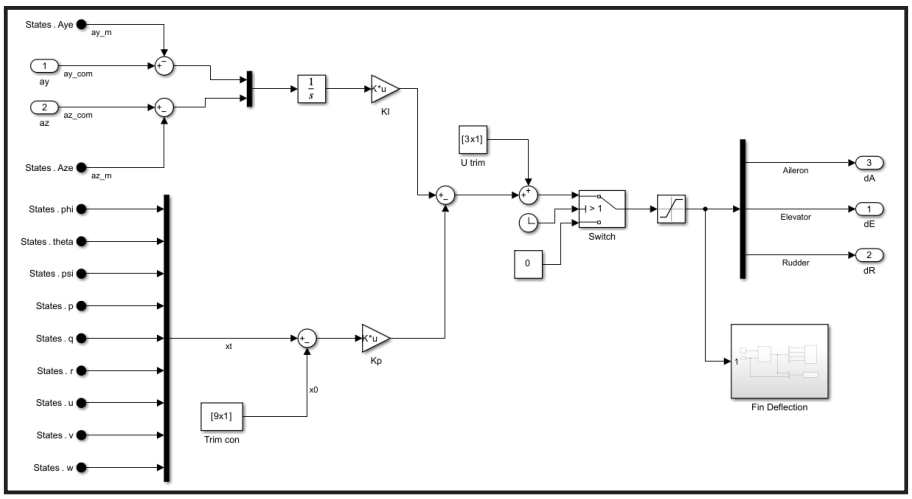

Figure 14: Simulink Model of Missile Control System.

The feedback variables, as shown in Figure 2-12, are all the states and two missile lateral accelerations, a_{y_b} and a_{z_b}. The missile lateral acceleration is fed back to the control system to follow the commanded acceleration from proportional navigation guidance.

The LQR method is applied to the state error equation to obtain the gain matrix. The values of Q and R used are,

$$\boldsymbol{Q} = \begin{bmatrix} 1000 & 0 & 0 & 0 & 0 & 0 & 0 & 0 & 0 & 0 & 0 \\ 0 & 1 & 0 & 0 & 0 & 0 & 0 & 0 & 0 & 0 & 0 \\ 0 & 0 & 1 & 0 & 0 & 0 & 0 & 0 & 0 & 0 & 0 \\ 0 & 0 & 0 & 1 & 0 & 0 & 0 & 0 & 0 & 0 & 0 \\ 0 & 0 & 0 & 0 & 1 & 0 & 0 & 0 & 0 & 0 & 0 \\ 0 & 0 & 0 & 0 & 0 & 1 & 0 & 0 & 0 & 0 & 0 \\ 0 & 0 & 0 & 0 & 0 & 0 & 1 & 0 & 0 & 0 & 0 \\ 0 & 0 & 0 & 0 & 0 & 0 & 0 & 1 & 0 & 0 & 0 \\ 0 & 0 & 0 & 0 & 0 & 0 & 0 & 0 & 1 & 0 & 0 \\ 0 & 0 & 0 & 0 & 0 & 0 & 0 & 0 & 0 & 1000 & 0 \\ 0 & 0 & 0 & 0 & 0 & 0 & 0 & 0 & 0 & 0 & 1000 \end{bmatrix} \tag{32}$$

$$\boldsymbol{R} = \begin{bmatrix} 1 & 0 & 0 \\ 0 & 1 & 0 \\ 0 & 0 & 1 \end{bmatrix} \tag{33}$$

The values of Q(1,1), Q(10,10), and Q(11,11) were set to 1000 to prioritize roll stability and lateral acceleration tracking. A lower value may reduce the control system's responsiveness, while a higher value could lead to excessive control efforts and instability. In further development, the best Q value can be determined through trial-and-error simulations. The value chosen in the R matrix is 1, which corresponds to an identity matrix, because the three controllers are unconstrained.

The gain matrix $\widehat{\boldsymbol{K}}$ in equation (31) is obtained by the LQR method using the lqr function in Matlab. By using the Q matrix and R matrix as above, the gain matrix $\widehat{\boldsymbol{K}}$ is obtained as follows.

$$\widehat{\boldsymbol{K}} = \begin{bmatrix} 34.4 & 0 & 0.98 & 1.66 & 0 & -1.58 & 0 & -0.03 & 0 & -6.12 & 0 \\ 0 & -0.1 & 0 & 15.86 & 15.86 & 0 & 0.04 & 0 & 1.38 & 0 & 31.62 \\ 11.92 & 0 & -0.19 & 0 & 0 & 11.53 & 0 & -0.87 & 0 & -31.03 & 0 \end{bmatrix} \tag{34}$$

2.6. Numerical Modeling of Flight Simulation

Programming languages enable the designer to translate an algorithm into executable code. Usually, the main criterion for the software is that it is correct – it produces the correct

output to a defined accuracy (Allerton, 2009). The construction of a flight simulation model was conducted in Simulink, and it is essentially a system that describes Figure 1. This study was conducted under ideal conditions, neglecting factors such as noise, response delays, and system uncertainties. The flight simulation model shown in Figure 15 consists of several subsystems: Target, Range, Proportional Navigation, Flight Control, and Missile Dynamics. The Target subsystem represents the target's motion. The Range subsystem computes the range of the missile and the target. The Proportional Navigation subsystem determines the geometry between target and missile and then computes the acceleration command using the proportional navigation equation. The Flight Control subsystem determines the deflection of the control surfaces to achieve commanded acceleration. The Missile Dynamics subsystem represents the flight dynamics of the missile, which is the motion of the missile.

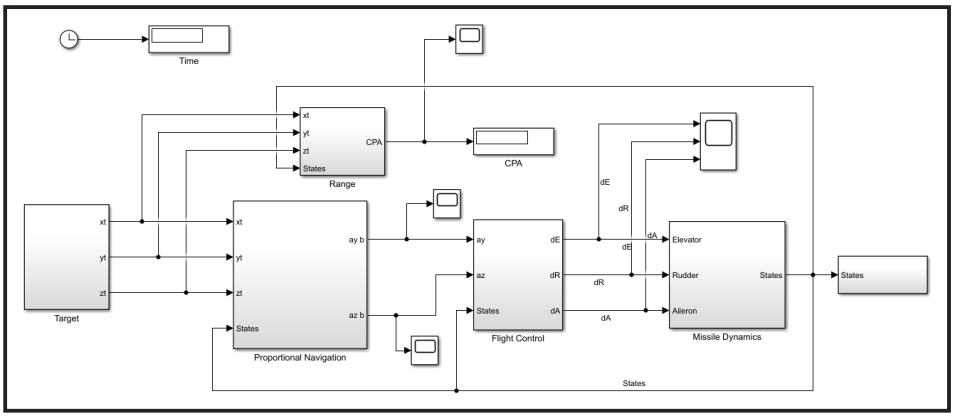

Figure 15: Flight Simulation Model in Simulink.

3. Result and Analysis

The simulation was conducted in various target conditions and with zero initial velocity for each case. Four aspects are varied, which are target direction, target maneuver in pitch plane, target maneuver in yaw plane, and target maneuver in both pitch and yaw plane.

3.1. Target Direction Variation

The target direction is the angle of velocity direction with respect to the local horizon axis in the yaw plane. To analyse the variations of the target direction, the target was set to have a height of 5 km, a horizontal distance of 5 km, and a constant speed of 200 m/s. The variations of the yaw direction angle of the target are $\gamma_{t_{yaw}} = 0°, 45°, 90°$, and $180°$. The target direction $\gamma_{t_{yaw}} = 0°$ is the tail-chase scenario and $\gamma_{t_{yaw}} = 180°$ is a head-on engagement. After carrying out the simulation, the following results were obtained.

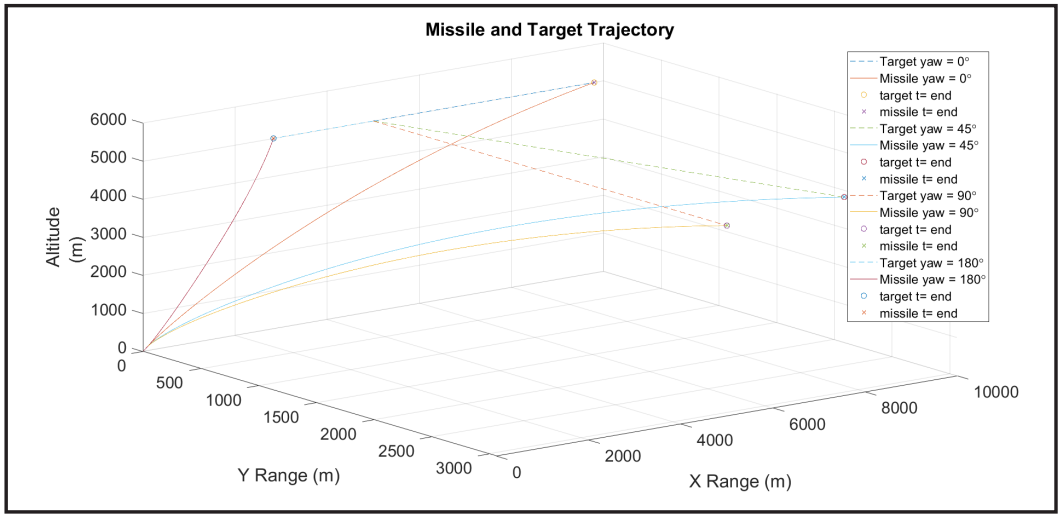

Figure 16: Missile and Target Trajectory with The Variation of Target Direction.

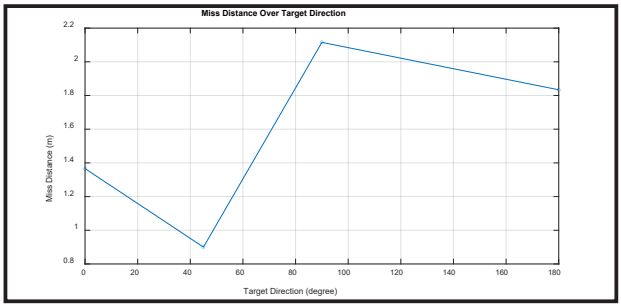

Figure 17: Miss Distance of Engagements with The Variation of Target Direction.

Figure 16 shows the missile trajectory and the target with variations in target yaw direction. Figure 17 shows the miss distance for each engagement. From these graphs, it can be shown that the missile can intercept the target in all variations of the target yaw direction.

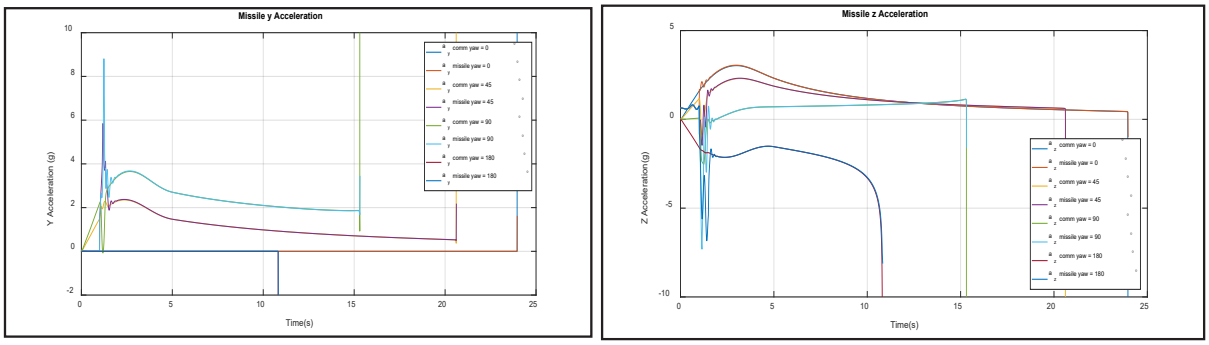

(a) (b)

Figure 18: (a) Missile Acceleration and Acceleration Command in Y axis (b) Missile Acceleration and Acceleration Command in Z axis.

Figure 18 illustrates the missile acceleration and missile acceleration commands in the y-axis and z-axis. In variations of the target yaw direction at 0° and 180°, the missile acceleration command is only present in the z-axis, as in these directions, the target is situated on a single plane.

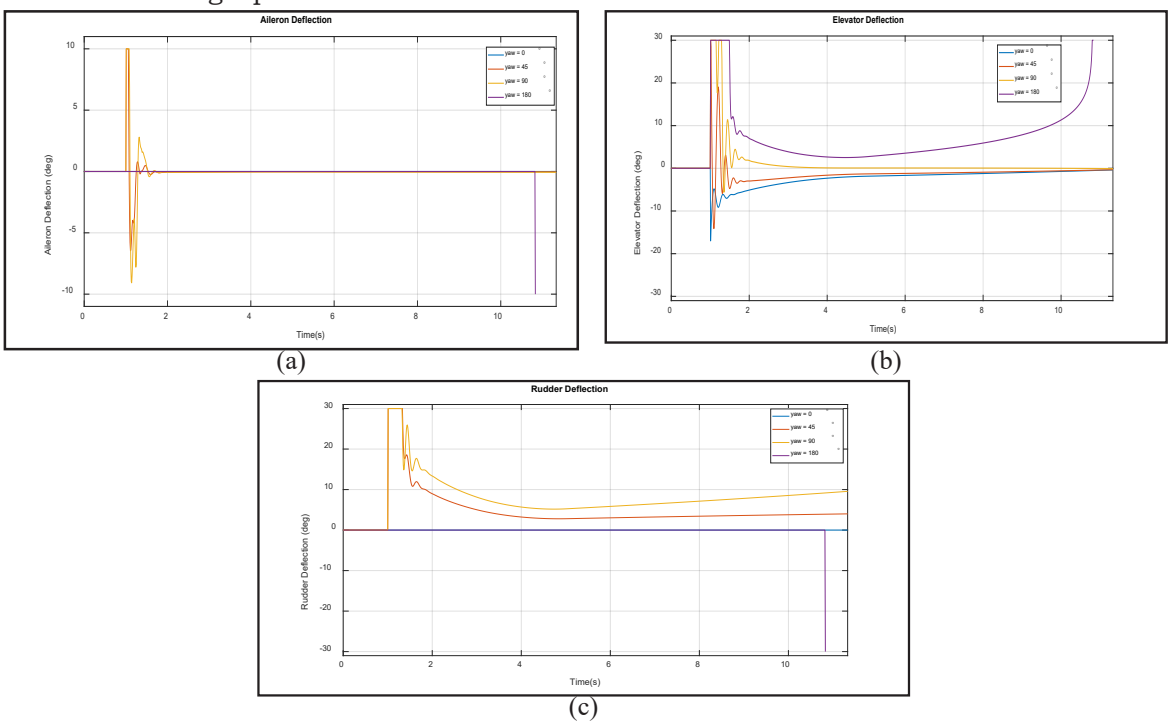

(a) (b)

(c)

Figure 19: (a) Aileron Deflection, (b) Elevator Deflection, (c) Rudder Deflection.

Figure 3-4 illustrates the control surface deflections for each variation of the target yaw direction. It can be observed that for variations in the target yaw direction at $0°$ and $180°$, the aileron and rudder are not deflected because the target is situated on a single plane. In variations of the target yaw direction at $45°$ and $90°$, all control surfaces are deflected since the target is positioned in two planes (pitch and yaw planes). The aileron is deflected as well because when the missile moves in two planes, there is a roll moment.

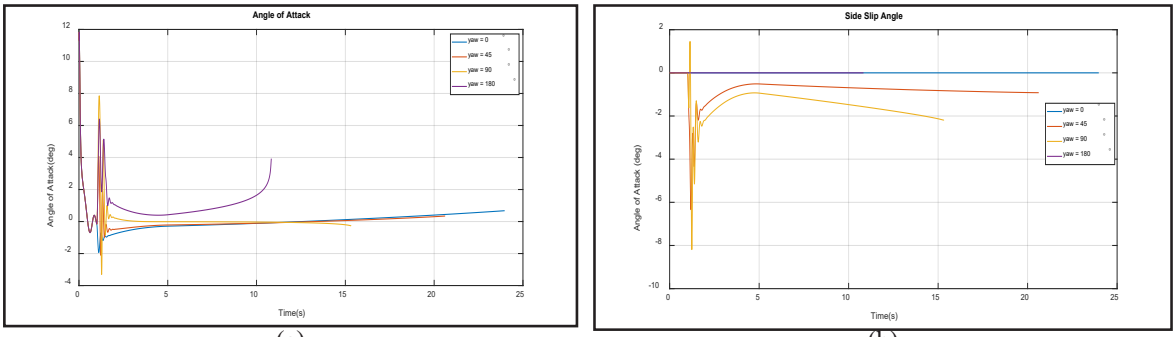

(a) (b)

Figure 20: (a) Angle of Attack and (b) Side Slip Angle with Variation of Target Direction.

Figure 3- 5 illustrates the variation of the missile's angle of attack (AoA) and the missile's side-slip angle (β) over time for different target yaw direction. For all the variations of target yaw direction, these have relatively small AoA oscillation at the beginning of engagement before it stabilises. At a target yaw of 180°, the AoA increases from mid-engagement to the end, indicating that this engagement requires the highest maneuvre. At target yaw of $0°$ and $180°$, there is no side-slip angle, indicating purely axial motion with no lateral deviation. In the target yaw of $45°$ and $90°$, the missile initially experiences high oscillations in β due to the abrupt need for lateral course adjustments.

3.2. Target Maneuver Variation in Pitch Plane

The target maneuver is the target turn in the pitch or yaw plane. The measurement of the target maneuver is the acceleration experienced by the pilot. To analyze the variations of the target maneuver in the pitch plane, the target was set to have a height of 5 km, a horizontal distance of 5 km, and a constant speed of 200 m/s towards the approaching target. The variations of the target maneuver acceleration in the pitch plane are $a_{t_z} = 3g, 5g, 7g,$ and $8g$. After carrying out the simulation, the following results were obtained.

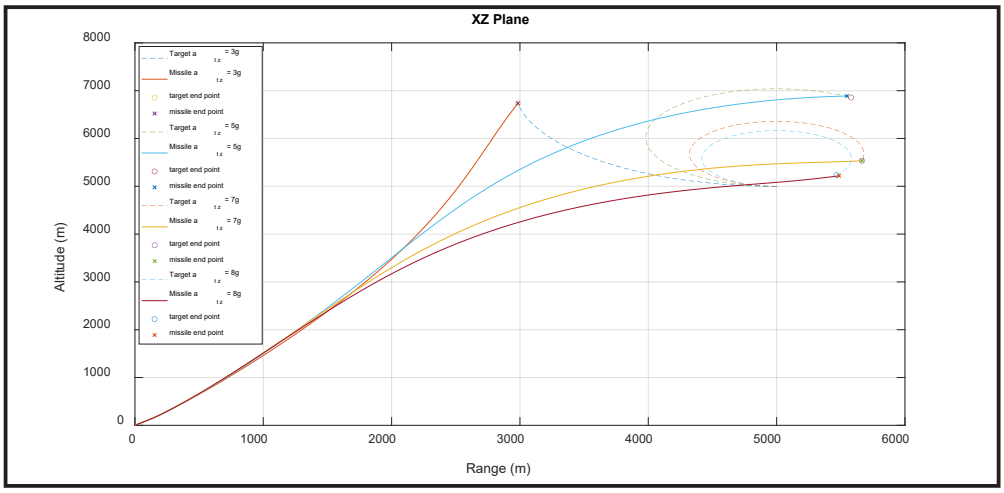

Figure 21: Missile and Target Trajectories with Target Maneuver Variation in the Pitch Plane.

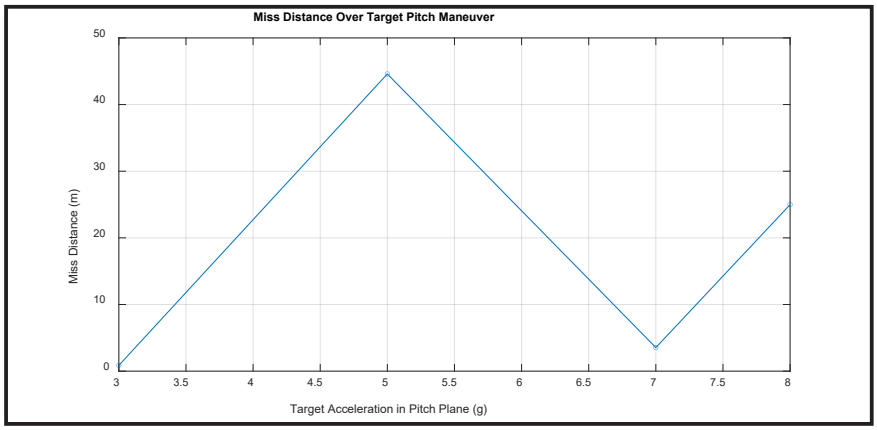

Figure 22*:* Miss Distance of Engagements with The Variation of Target Pitch Maneuver.

Figure 21 illustrates the missile trajectory with variations in the target's pitch maneuver. Figure 22 shows the miss distance for each engagement. In these figures, it is evident that the missile's endpoint is close to the target. Targets with maneuvers of 3g were successfully intercepted. When magnified, it can be observed that targets with maneuvers of 5g and 8g were not successfully intercepted due to their shorter distances.

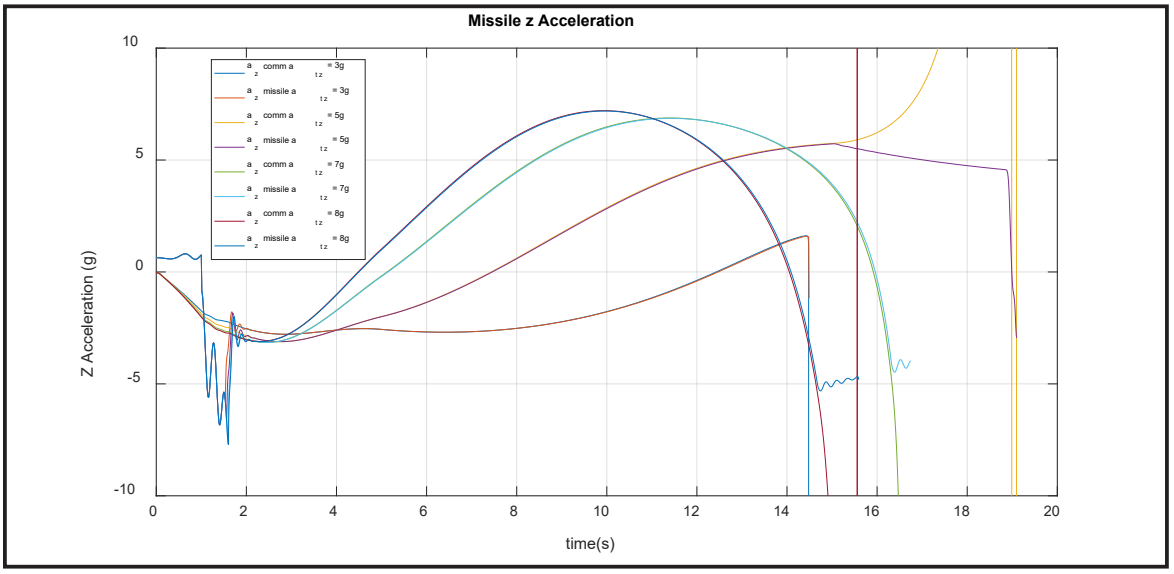

Figure 23: Missile Acceleration and Acceleration Command in Z axis.

Figure 23 depicts the acceleration command and missile acceleration. It can be observed that for targets with maneuvers of 3g and 7g, the missile can accurately follow the acceleration command. For targets with maneuvers of 5g and 8g, the missile can initially follow the acceleration command well. However, towards the end of the trajectory, the missile cannot maintain the acceleration command, resulting in a miss of the target. This limitation arises due to the combination of aerodynamic control authority and the missile's available lateral acceleration capability. As the target's acceleration increases, the missile requires higher control deflections to maintain intercept trajectories, which may exceed the aerodynamic limits of the missile fins.

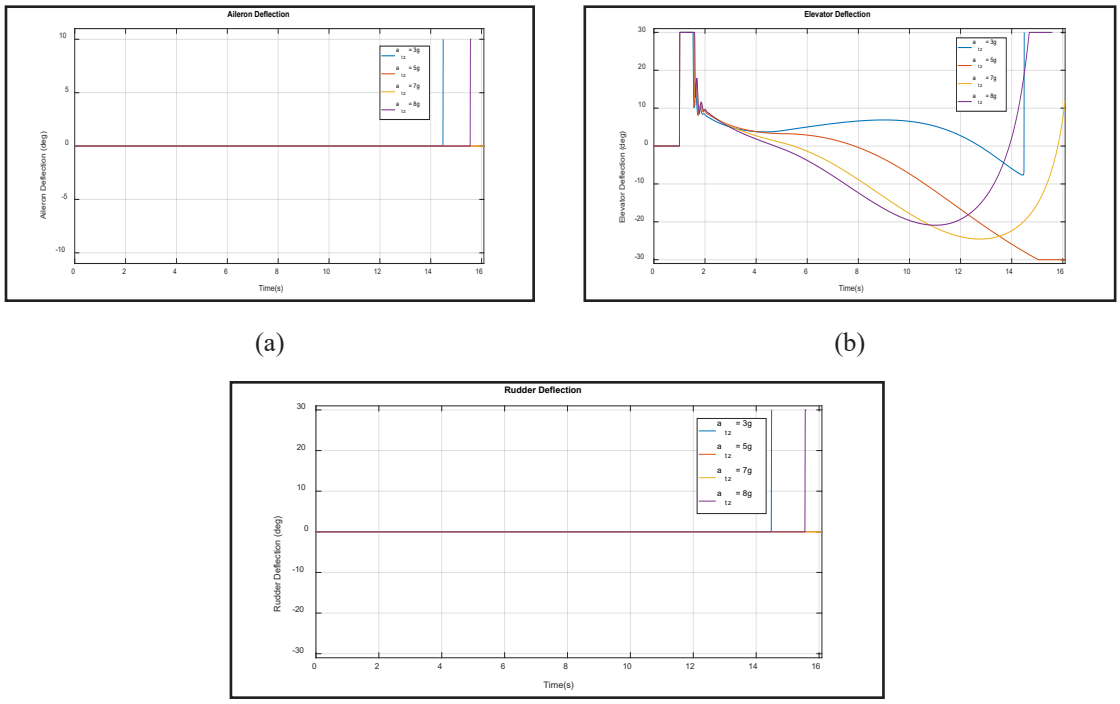

(a) (b)

(c)

Figure 24: (a) Aileron Deflection, (b) Elevator Deflection, (c) Rudder Deflection.

Figure 24 shows the control plane deflection for each variation of the target maneuver. The aileron and rudder deflection commands are zero because the missile only moves in the pitch plane; deflection only occurs at the elevator.

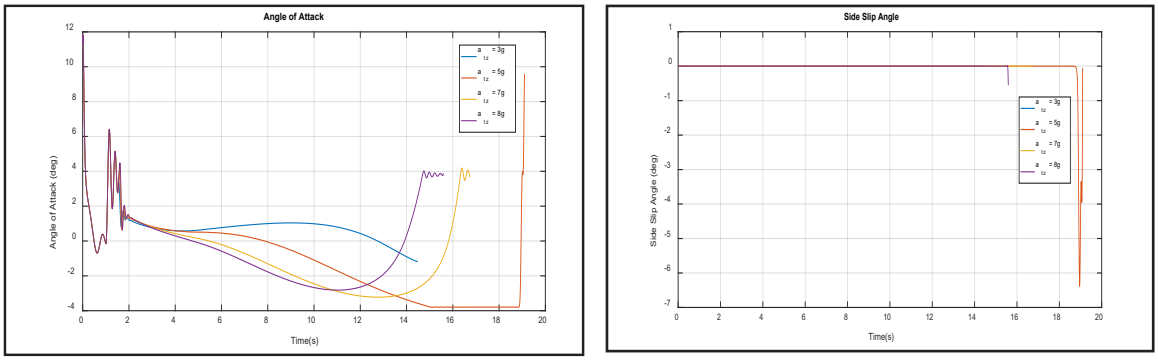

(a) (b)

Figure 25: (a) Angle of Attack, (b) Side Slip Angle with variation of Target Pitch Maneuver.

Figure 25 illustrates the variation of the missile's angle of attack (AoA) and the missile's side-slip angle (β) over time for different target pitch maneuver. For all the variations of target pitch maneuver, the missile initially experiences oscillations in AoA and then varies depending on the missile's Z acceleration. There is no side-slip angle for all variations of the target pitch maneuver, except at the end of the engagement, which indicates no lateral deviation.

3.3. Target Maneuver Variation in Yaw Plane

To analyze the variations of the target maneuver in the yaw plane, the target was set to have a height of 5 km, a horizontal distance of 5 km, and a constant speed of 200 m/s towards the approaching missile. The variations of the target maneuver acceleration in the yaw plane are $a_{t_y} = 3g, 4g,$ and $5g$. After carrying out the simulation, the following results were obtained.

Figure 26 shows the trajectory of the missile and target with variations in the yaw plane target maneuver. Figure 26 shows the miss distance for each engagement. These

graphs show that the missile is capable of intercepting targets with 3g and 4g maneuvers in the yaw plane. On targets with 5g maneuvers, the missile can approach the target but not close enough for the missile to miss.

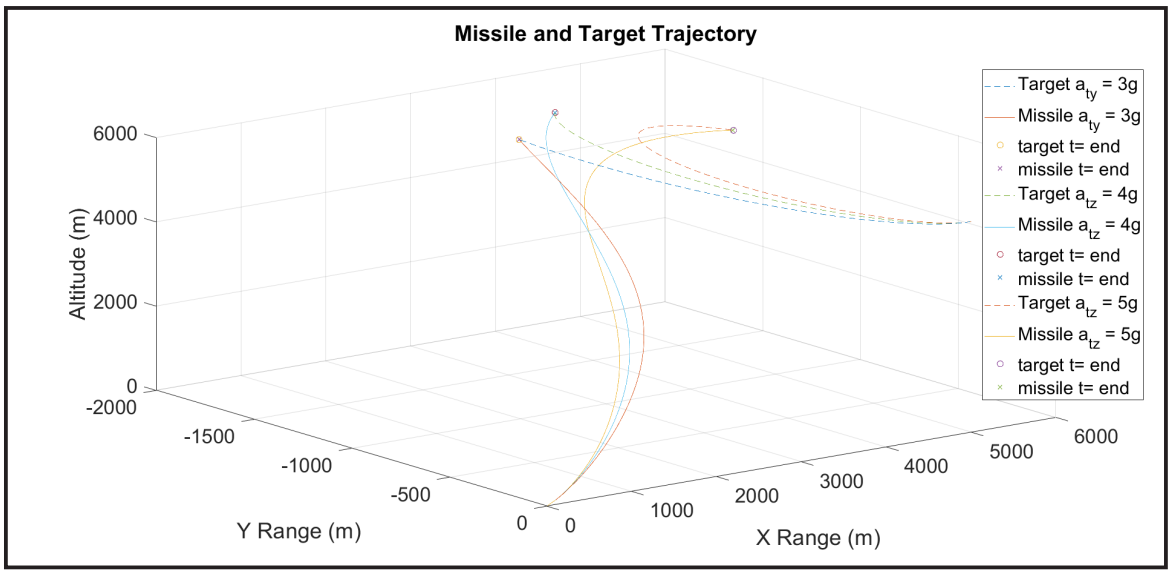

Figure 26: Missile and Target Trajectory in Three-Dimensional Space.

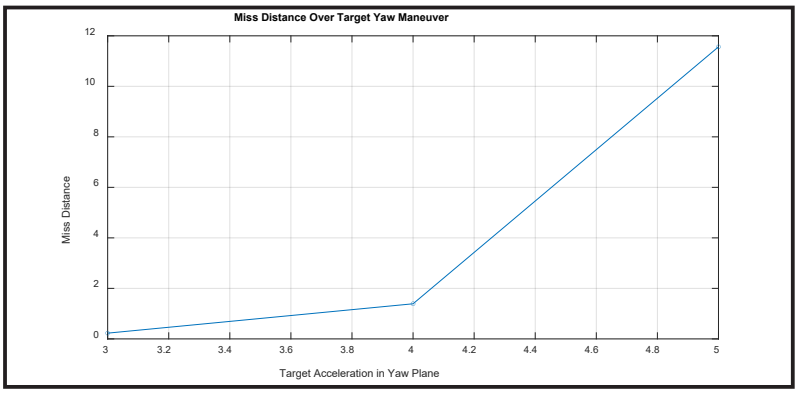

Figure 27*:* Miss Distance of Engagements with The Variation of Target Pitch Maneuver.

Figure 28 shows the acceleration of the missile in the y-axis and z-axis. For y acceleration, the missile can follow the acceleration command; however, on targets with 4g and 5g maneuvers at the end of the second, the missile has difficulty following the acceleration command. The acceleration command in 5g maneuvers is tremendous, and the rapid change causes the missile to fail to keep up and ultimately miss the target. Similar to the previous simulation in section 3.2, this limitation is due to aerodynamic control authority and the missile's available lateral acceleration capability.

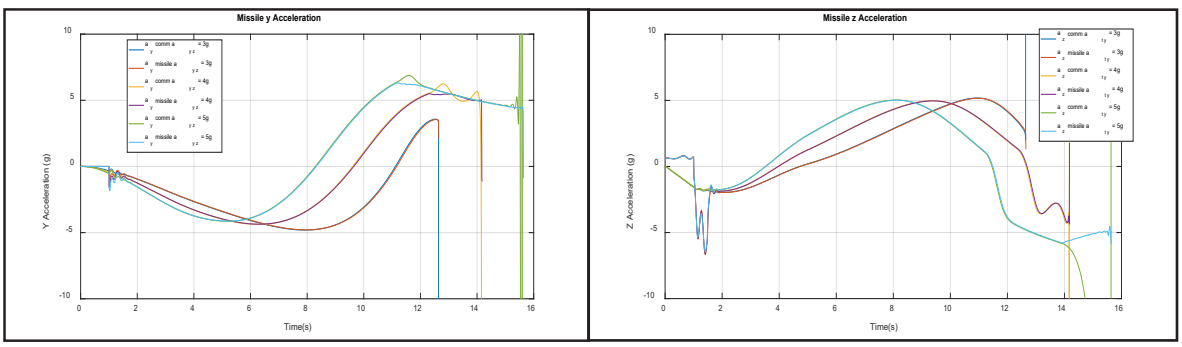

(a) (b)

Figure 28: (a) Missile Acceleration and Acceleration Command in Y Axis, (b) Missile Acceleration and Acceleration Command in Z Axis.

Figure 29 illustrates the control plane deflection for each variation of the target ma-

neuver. The resulting elevator deflection and rudder deflection are maximum when the control is applied at the start and at the end of the time.

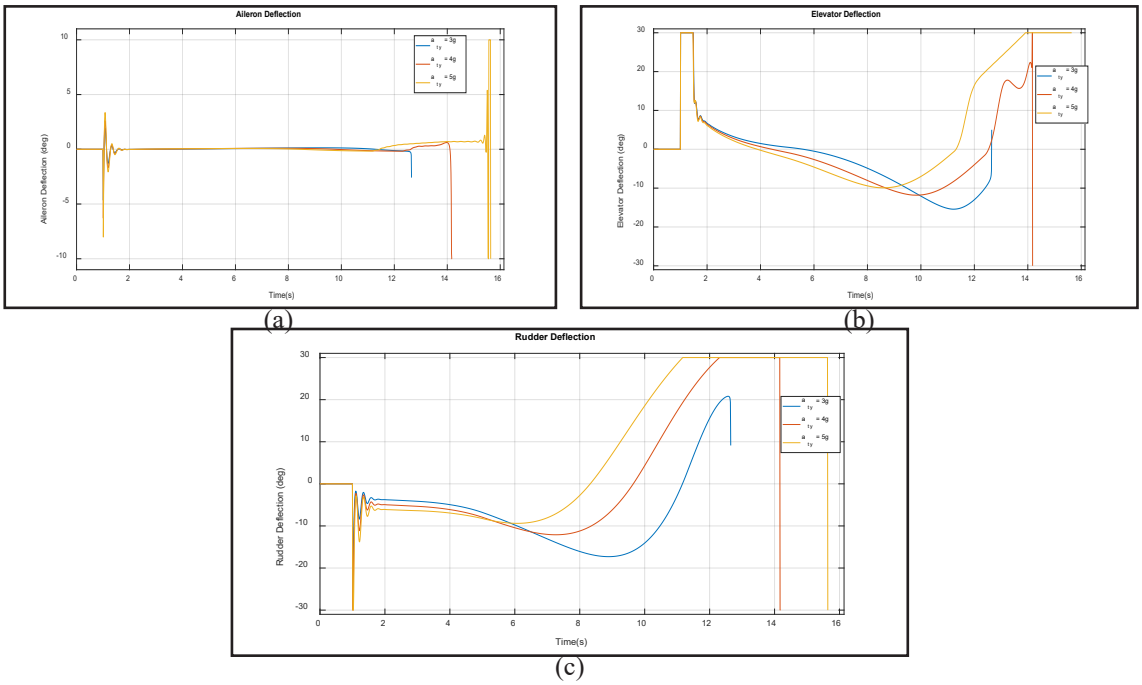

(a) (b)

(c)

Figure 29: (a) Aileron Deflection, (b) Elevator Deflection, (c) Rudder Deflection.

Figure 30 illustrates the variation of the missile's angle of attack (AoA) and the missile's side-slip angle (β) over time for different target yaw maneuver. Initially, all cases exhibit a sharp peak in both AoA and β, with higher target acceleration values (5g) experiencing more pronounced fluctuations due to greater maneuvering forces. After the initial disturbances, the AoA and β stabilize but follows distinct trajectories based on the target's maneuver intensity.

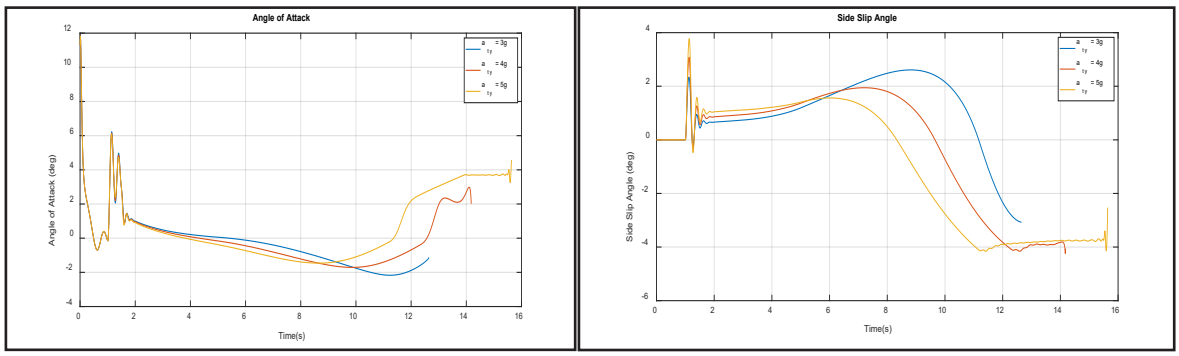

(a) (b)

Figure 30: (a) Angle of Attack, (b) Side Slip Angle with variation of Target Yaw Maneuver.

3.4. Target Maneuver Variation in Both Pitch and Yaw Planes

To analyze the variations of the target manoeuvre in both pitch and yaw planes, the target was set to have a height of 5 km, a horizontal distance of 5 km, and a speed of 200 m/s towards the approaching direction. The variations of the target total maneuver acceleration are $a_t = 3g, 4g,$ and $5g$. After carrying out the simulation, the following results were obtained.

Figure 3-16 shows the trajectory of the missile and target with variations in the pitch-yaw plane target manoeuvre. Figure 3-17 shows the miss distance for each engagement. From these graphs, it can be seen that with 3g and 4g maneuvers, the missile can intercept the target. On targets with 5g maneuvers, the missile can approach the target, but at the

end point, the missile is not close enough to the target, so it is considered to have missed.

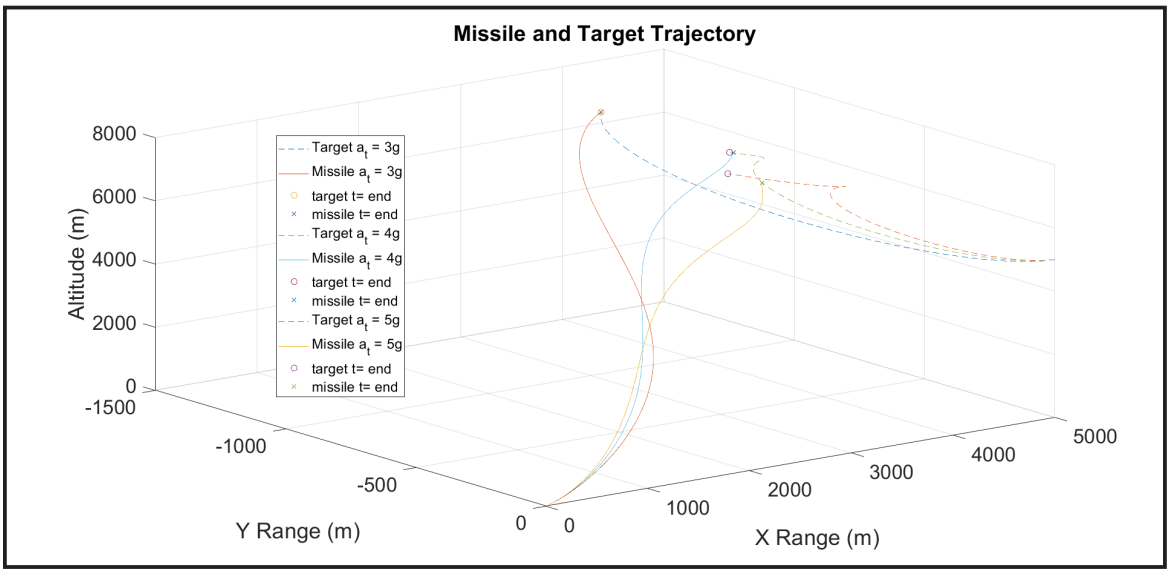

Figure 31: Missile and Target Trajectory with Variation of Target Maneuver in Both Pitch and Yaw Planes.

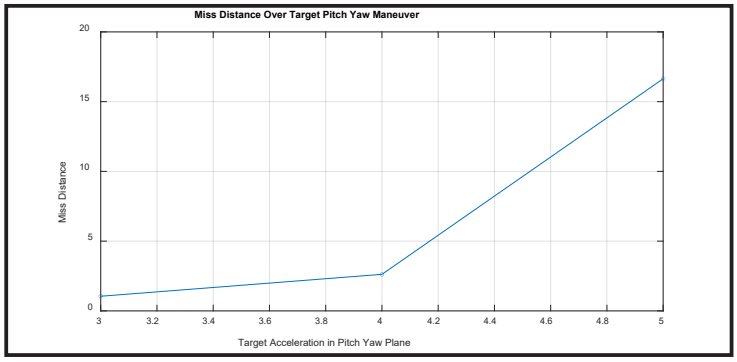

Figure 32: Miss Distance of Engagements with The Variation of Target Pitch Maneuver.

Figure 33 shows the acceleration of the missile in the y-axis and z-axis. For the y acceleration, the missile can follow the acceleration command. However, on targets with a 5g maneuver at the end of the second, the missile has difficulty following the acceleration command, as the other results in Section 3.2.

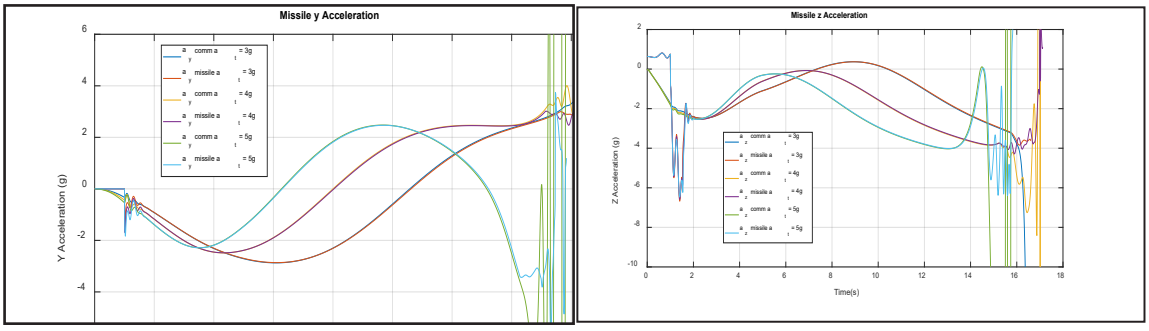

(a) (b)

Figure 33: (a) Missile Acceleration and Acceleration Command in Y axis, (b) Missile Acceleration and Acceleration Command in Z Axis.

Figure 34 shows the control plane deflection for each variation of the target maneuver. The resulting elevator deflection and rudder deflection are maximum when the control is applied at the start and at the end of the second.

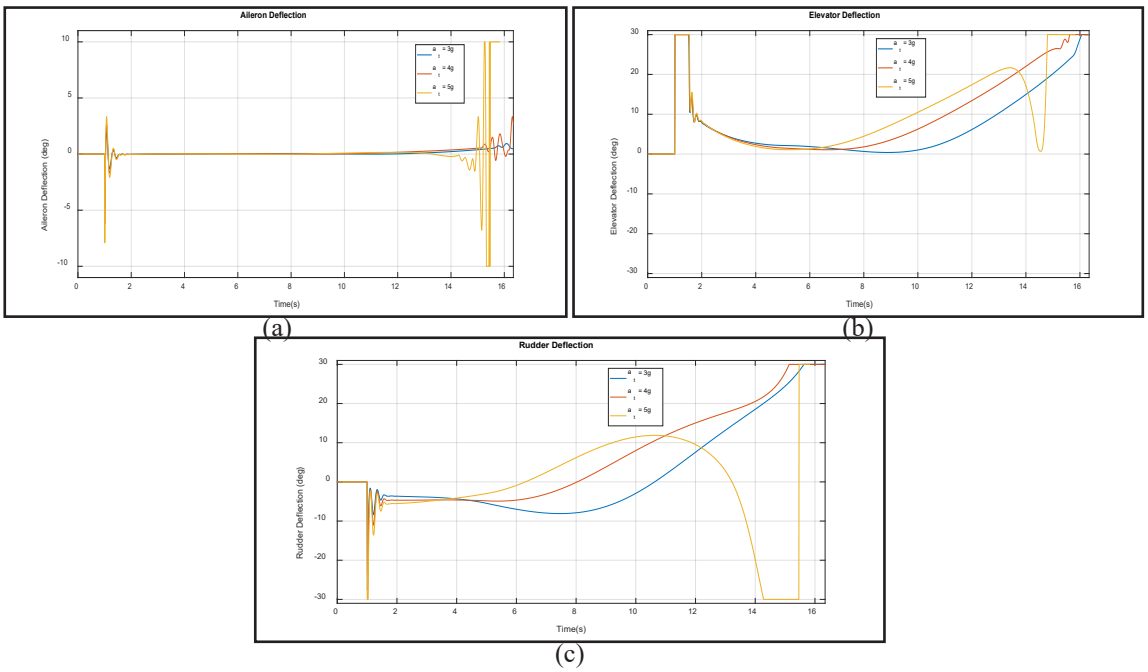

(a) (b) (c)

Figure 34: (a) Aileron Deflection, (b) Elevator Deflection, (c) Rudder Deflection.

Figure 35 illustrates the variation of the missile's angle of attack (AoA) and the missile's side-slip angle (β) over time for a different target pitch yaw maneuver, showing that higher target accelerations (4g and 5g) lead to greater aerodynamic disturbances. Initially, all cases exhibit transient oscillations before stabilizing, but as the engagement progresses, higher target maneuvers cause increased AoA and β variations. The 5g case shows significant instability near the end point, indicating aerodynamic challenges that could affect missile control.

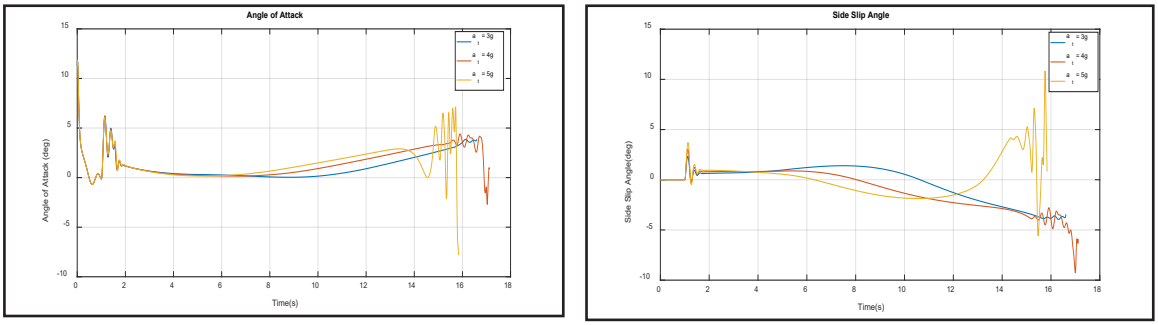

(a) (b)

Figure 35: (a) Angle of Attack, (b) Side Slip Angle with variation of Target Pitch Yaw Maneuver.

4. Conclusion

In conclusion, this paper presents a comprehensive study on the development of a guided missile, specifically a surface-to-air missile, utilizing a 122mm rocket as its basis. The research involves modeling missile dynamics, guidance systems, and control systems, with a focus on constructing a missile guidance and control system using Simulink software. The results show that the missile can intercept a non-manoeuvring target at a distance of 5 km and a height of 5 km, which flies in various directions. The missile can also intercept a maneuverable target that maneuver in pitch plane, yaw plane, and both pitch and yaw planes up to 4g. However, the missile failed to intercept a high maneuverability target which can maneuver by 5g or more. This limitation arises due to the combination of aerodynamic control authority and the missile's available lateral acceleration capability. In further development, it can be improved by increasing control surface effectiveness by modifying fin size and deflection range, while implementing adaptive or nonlinear control

e-ISSN 2597-7873 (online) | © 2025 The Author(s). Published by BRIN Publishing.

IJOA accredited as Sinta 2 Journal (https://sinta.kemdikbud.go.id/journals/profile/3362)

methods to improve high-g maneuver tracking. These results indicate that the 122mm caliber rocket used in this simulation is potentially suitable for development as a SAM.

Acknowledgements

The authors would like to thank everyone who helped with this research paper. Their support and advice were significant. The authors would especially like to thank their advisors, Rianto Adhy Sasongko, Ph.D., Dr. Taufiq Mulyanto, and Y. H. Yogaswara, Ph.D., for their constant support, guidance, and helpful feedback, which played a crucial role in making this project successful by fostering a collaborative and excellent research atmosphere.

Contributorship Statement

AA is the main contributor to this research by developing the simulation model, conducting the simulation, and analyzing the simulation results. YHY contributed to the missile data, algorithm of missile dynamics, guidance, control, and simulation, supervising the manuscript and suggesting improvements; RAS and TM guided, supervised, and suggested improvements for the research.

References

Allerton, D. (2009). Principles of Flight Simulation. West Sussex: John Wiley & Sons, Ltd.

Ardiansyah, A. (2022). Simulasi Titik Massa Panduan Proportional Navigation dan Pemilihan FINSET untuk SAM Berbasis R-Han 122B Menggunakan Simulink dan Missile Datcom. Bandung: Institut Teknologi Bandung.

Cahyono, A. M., Navalino, R. A., & Yogaswara, Y. (2021). Analisis Persyaratan dan Tingkat Kesiapterapan Teknologi Sistem Senjata Roket Balistik R-Han 122B Untuk Pertahanan Indonesia. Jurnal Teknologi Persenjataan, 32-48.

Costello, P. (1995). Simulink simulation of proportional navigation and command to line of sight guidance. California: Calhoun Institutional Archive of the Naval Postgraduate School.

Fleeman, E. L. (2001). Tactical Missile Design. Reston, Virginia: AIAA.

Hibbeler, R. C. (2010). Engineering Mechanics: dynamics (12 ed.). Upper Saddle River, New Jersey: Pearson Prentice Hall.

Lukenbill, F. C. (1990). A target missile engagement scenario using classical proportional navigation. Institutional Archive of the Naval Postgraduate School. Monterey: Naval Postgraduate School. Retrieved from https://calhoun.nps.edu/handle/10945/27627

Membangun Kembali Satuan Rudal TNI AU. (2021, April 16). Retrieved from Kemen-

terian Pertahanan Republik Indonesia: https://www.kemhan.go.id/baranahan/2021/04/16/membangun-kembali-satuan-rudal-tni-au.html

Meriam, J. L., Kraige, L., & Bolton, J. (2015). Engineering Mechanics : dynamics (8 ed., Vol. 2). John Wiley & Sons, Inc.

Mulder, J. A., Staveren, W. v., van der Vaart, J., & Weerdt, E. (2011). Flight Dynamics. Delft: Delft University of Technology.

Ogata, K. (2010). Modern Control Engineering (5th ed.). New Jersey: Prentice Hall.

R-Han 122.(2022, November 26). Retrieved from Wikipedia: https://id.wikipedia.org/wiki/R-Han_122

Rosema, C., Doyle, J., Underwood, M., & Auman, L. (2011). Missile Datcom User's manual. Air Force Research Laboratory.

Siouris, G. M. (2004). Missile Guidance and Control Systems. New York: Springer-Verlag.

Yogaswara, Y. H. (2020, June). Rancangan Konsep Misil Permukaan-ke-Udara Berbasis Roket Kal. 122 Sebagai Senjata Penindak Dalam Operasi Gabungan Pertahanan Udara. Karya Tulis Ilmiah Kategori Alutsista.